Supporting Information

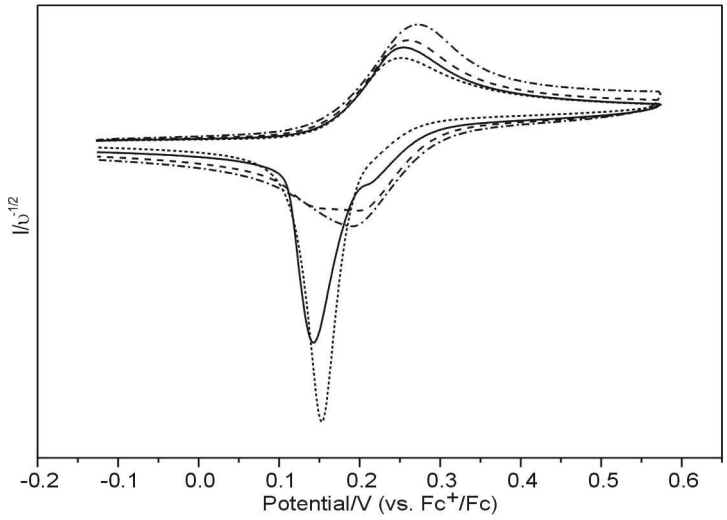

Figure S1 Cyclic voltammograms recorded for **1a** in CH_2Cl_2 containing $[Bu_4N][BF_4]$ (0.4 M) showing the effect of scan rate on profile of the oxidation process. 0.02 Vs^{-1} (short dashed line), 0.10 Vs^{-1} (solid line), 0.20 Vs^{-1} (dashed line), and 0.50 Vs^{-1} (dashed-dotted line).

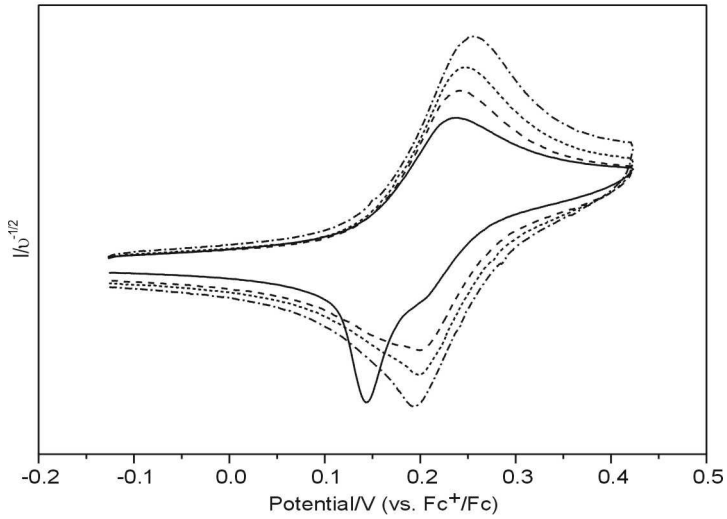

Figure S2. Cyclic voltammograms recorded for **1a** in CH_2Cl_2 containing $[Bu_4N][BF_4]$ (0.4 M) showing the effect of scan rate on profile of the oxidation process. 0.10 Vs^{-1} (solid line), 0.50 Vs^{-1} (dashed line), 1.00 Vs^{-1} (short dashed line) and 2.00 Vs^{-1} (dashed-dotted line).

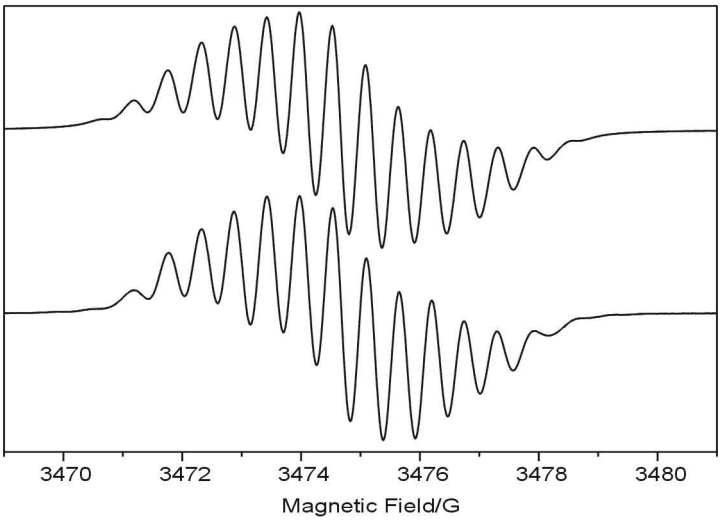

Figure S3. Experimental (bottom) and simulated (top) EPR spectra for electrochemically generated **1a**$^{-}$ in CH_2Cl_2 containing $[Bu_4N][BF_4]$ (0.4 M) at 291 K.

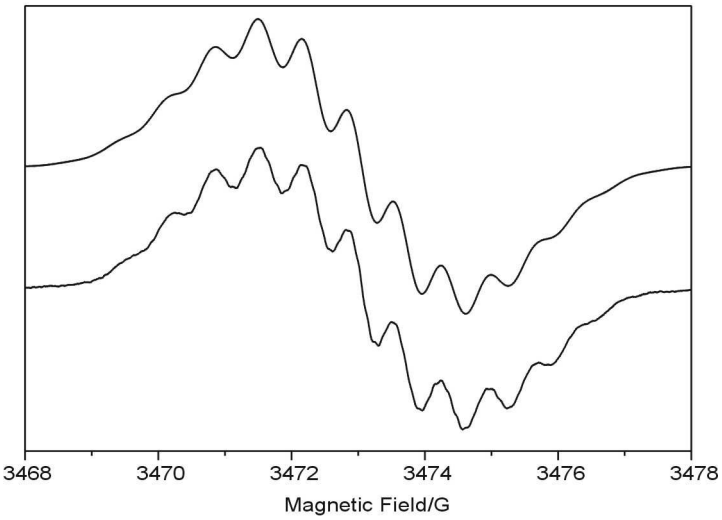

Figure S4. Experimental (bottom) and simulated (top) EPR spectra for electrochemically generated **2**$^{-}$ in CH_2Cl_2 containing $[Bu_4N][BF_4]$ (0.4 M) at 291 K.

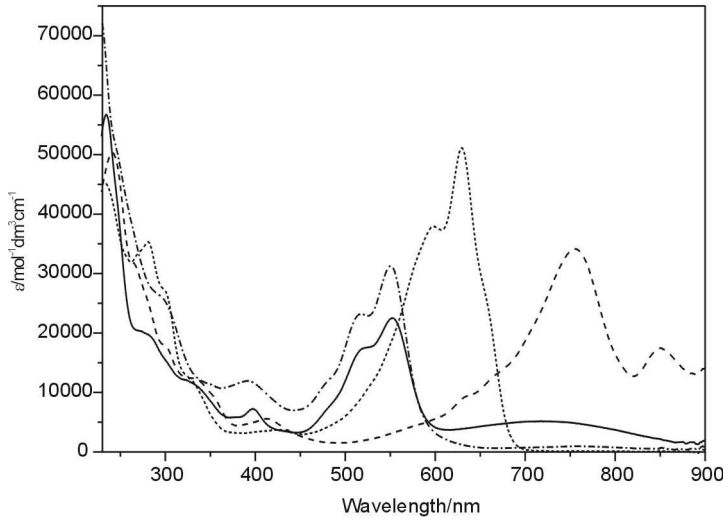

Figure S5. UV-visible spectra recorded in CH_2Cl_2 containing $[Bu_4N][BF_4]$ (0.4 M) using spectroelectrochemical methods for **2** at 273 K. The spectrum of **2** is represented by the solid line, $\mathbf{2}^-$ (dashed line), $\mathbf{2}^{2-}$ (short dashed line) and the oxidised species $\mathbf{2}^{2+}$ recorded at 243 K (dashed-dotted line).

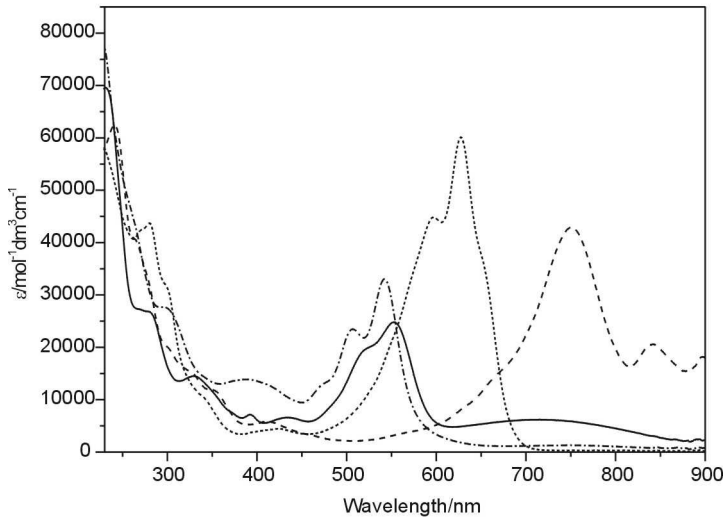

Figure S6. UV-visible spectra recorded in CH_2Cl_2 containing $[Bu_4N][BF_4]$ (0.4 M) using spectroelectrochemical methods for **3** at 273 K. The spectrum of **3** is represented by the solid line, $\mathbf{3}^-$ (dashed line), $\mathbf{3}^{2-}$ (short dashed line) and the oxidised species $\mathbf{3}^{2+}$ recorded at 243 K (dashed-dotted line)

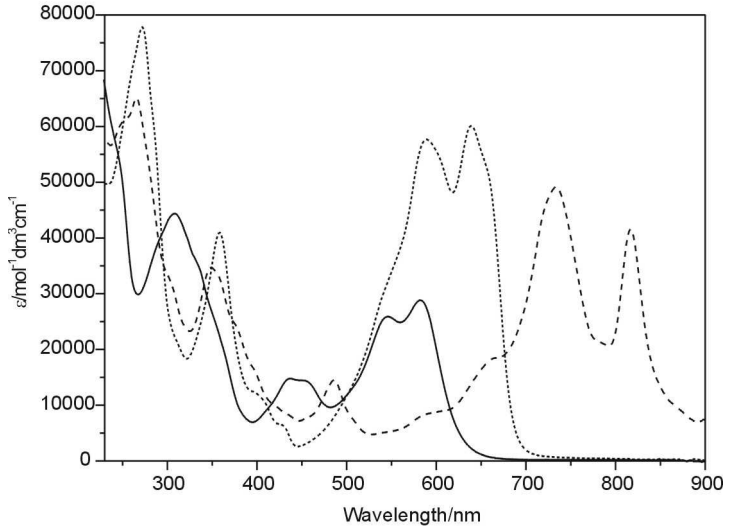

Figure S7. UV-visible spectra recorded in CH_2Cl_2 containing $[Bu_4N][BF_4]$ (0.4 M) using spectroelectrochemical methods for **5** at 273 K. The spectrum of **5** is represented by the solid line, $\mathbf{5}^-$ (dashed line) and $\mathbf{5}^{2-}$ (short dashed line).

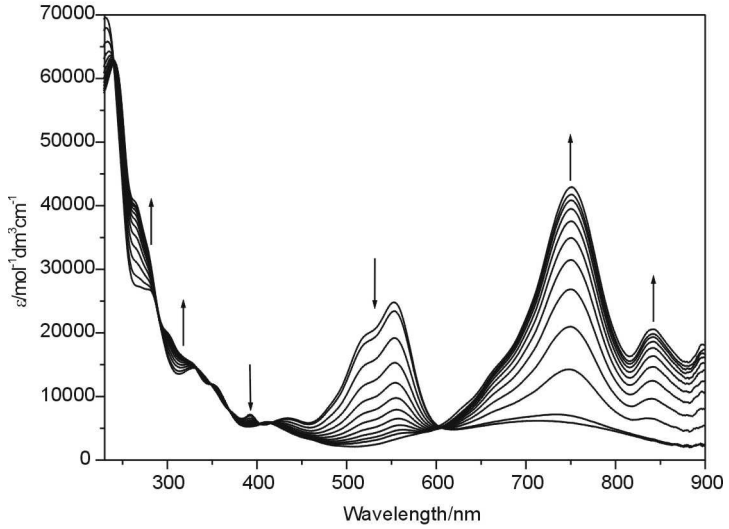

Figure S8. UV-visible spectra recorded in CH_2Cl_2 containing $[Bu_4N][BF_4]$ (0.4 M) using spectroelectrochemical methods for **3** at 273 K showing the inter-conversion of **3** to $\mathbf{3}^-$. Arrows indicate the progress of the reduction.

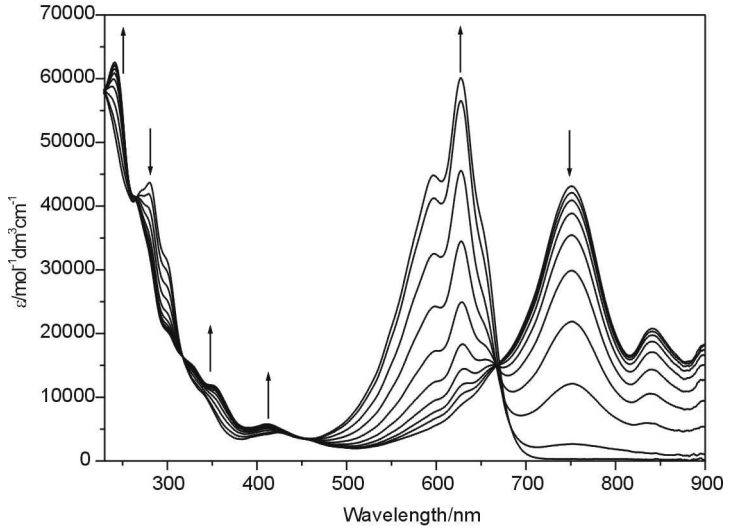

Figure S9. UV-visible spectra recorded in CH_2Cl_2 containing $[Bu_4N][BF_4]$ (0.4 M) using spectroelectrochemical methods for **3** at 273 K showing the inter-conversion of $\mathbf{3}^{-}$ to $\mathbf{3}^{2-}$. Arrows indicate the progress of the reduction.

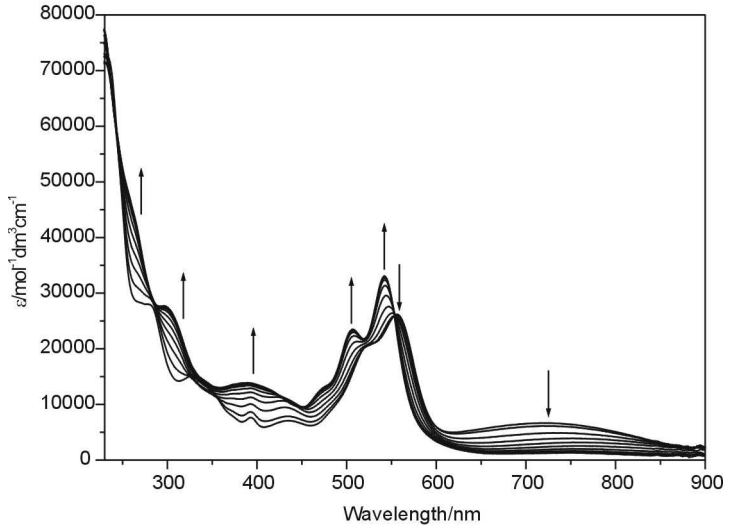

Figure S10. UV-visible spectra recorded in CH_2Cl_2 containing $[Bu_4N][BF_4]$ (0.4 M) using spectroelectrochemical methods for **3** at 273 K showing the interconversion of **3** to $\mathbf{3}^{2+}$. Arrows indicate the progress of the oxidation.

Table S1. UV-visible spectroelectrochemical data for disubstituted PBI derivatives **1**-**5** in neutral, reduced and oxidised.

Compound	λ_{max}/nm (ε/moldm^{-3}cm^{-1})
[**1a**]^{0}	307 (2.9), 431 (1.2), 523 (1.8), 556(2.4), 686 (0.7)
[**1a**]$^{1-}$	245 (6.2), 348 (2.7), 460 (0.8), 736 (3.9), 825 (3.0)
[**1a**]$^{2-}$	243 (6.1), 274 (5.1), 342 (2.6), 429 (0.4), 589 (4.7), 634 (5.8)
[**1a**]$^{2+}$	234 (2.8), 299 (1.5), 416 (0.6), 523 (0.9), 561 (1.2), 766 (< 0.1)
[**2**]^{0}	235 (5.7), 398 (0.7), 552 (2.3), 718 (0.5)
[**2**]$^{1-}$	241 (5.1), 412 (0.6), 756 (3.5), 851 (1.8)
[**2**]$^{2-}$	232 (4.5), 281 (3.6), 598 (3.8), 630 (5.1)
[**2**]$^{2+\,b}$	391 (1.2), 518 (2.3), 551 (3.1), 760 (< 0.1)
[**3**]^{0}	329 (1.5), 392 (0.7), 434 (0.7), 553 (2.5), 711 (0.6)
[**3**]$^{1-}$	242 (6.3), 263 (4.1), 349 (1.2), 410 (0.6), 752 (4.3), 844 (2.1)
[**3**]$^{2-}$	280 (4.4), 295 (3.2), 424 (0.4), 596 (4.5), 628 (6.0)
[**3**]$^{2+\,b}$	295 (2.8), 388 (1.4), 506 (2.4), 542 (3.3)
[**4**]^{0}	293 (6.9), 466 (1.6), 600 (2.5)
[**4**]$^{1-}$	237 (7.1), 288 (6.4), 572 (1.6), 745 (4.1)
[**4**]$^{2-}$	236 (6.5), 288 (7.4), 600 (4.4)
[**4**]$^{4-}$	261 (6.9), 624 (5.0), 655 (3.5)
[**5**]^{0}	309 (4.4), 437 (1.5), 545 (2.6), 582 (2.9)
[**5**]$^{1-}$	266 (6.5), 348 (3.5), 486 (1.5), 734 (5.0), 817 (4.3)
[**5**]$^{2-}$	272 (7.8), 358 (4.1), 588 (5.8), 639 (6.0)

[a] in CH_2Cl_2 containing [$^{n}Bu_4N$][BF_4] (0.4 M) at 273 K unless stated otherwise, spectral range: 230 – 900 nm; [b] at 243 K